TITLE

Reactive Oxygen Detoxification Contributes to *Mycobacterium abscessus* Antibiotic Survival

AUTHORS

Nicholas A. Bates[1,2], Ronald Rodriguez[3,4], Rama Drwich[1], Abigail Ray[5], Sarah A. Stanley[3], Bennett H. Penn[1,6]*

AFFILIATIONS:

1. Department of Internal Medicine, University of California, Davis, California, USA
2. Graduate Group in Immunology, University of California, Davis, California, USA
3. Department of Molecular & Cell Biology, University of California, Berkeley, California, USA
4. Department of Plant & Microbial Biology, University of California, Berkeley, California, USA
5. Microbiology Graduate Group, University of California, Davis, California, USA
6. Department of Medical Microbiology and Immunology, University of California, Davis, California, USA

*Corresponding author

Email: bhpenn@ucdavis.edu

ABSTRACT

When a population of bacteria are exposed to a bactericidal antibiotic most cells die rapidly. However, a sub-population of antibiotic-tolerant cells known as “persister cells” can survive for prolonged periods, and antibiotic tolerance can be strongly induced in a population by stresses such as nutrient deprivation. However, the pathways required to maintain viability in this setting, and how they are regulated are poorly understood. To identify genetic determinants of antibiotic tolerance in mycobacteria, we carried out transposon mutagenesis insertion sequencing (Tn-Seq)

screens in *Mycobacterium abscessus* (*Mabs*) exposed to bactericidal translation-inhibiting antibiotics. This analysis identified genes essential for the survival of both spontaneous persister cells as well as for stress-induced tolerance, allowing the first genetic comparison of these states in mycobacteria. Pathway analysis identified multiple genes involved in the detoxification of reactive oxygen species (ROS), including the catalase-peroxidase *katG*, which contributed to survival in both stressed and un-stressed populations. In addition, we found that endogenous ROS were generated following antibiotic exposure, and that hypoxia significantly impaired bacterial killing. Thus, in *Mabs*, the lethality of some antibiotics is amplified by toxic ROS accumulation, and antibiotic-tolerant cells require detoxification systems to remain viable.

INTRODUCTION

A key goal of antibiotic therapy is, in conjunction with the immune system, to eradicate the infecting bacteria. While many common bacterial infections respond rapidly to antibiotics, with 1-2 weeks of therapy sufficient to achieve high cure rates, there are also infections where bacterial clearance is slow and often incomplete[1, 2]. This challenge is exemplified by mycobacterial infections. Fully-susceptible *Mtb* requires multiple antibiotics for four months or longer[3,4], and infections by non-tuberculous mycobacteria (NTM) such as *Mycobacterium abscessus* (*Mabs*) are often even more difficult to eradicate; *Mabs* often requires treatment for 12-18 months, and even then has a 50% relapse rate[5, 6].

While the ability of mycobacteria to escape antibiotic-mediated killing is multifactorial, the phenomenon of antibiotic tolerance is likely an important contributor[7-10]. Studies dating from the 1940s noted that when a population of susceptible bacteria were exposed to a bactericidal antibiotic such as penicillin, the majority of the population died within a few hours, but that a small sub-population of cells remained viable for days[11]. Importantly, these antibiotic-tolerant cells referred to as “persister cells” had not acquired a mutation conferring heritable antibiotic

53 resistance, and do not grow in the presence of the antibiotic. Rather, they had entered into a
54 readily-reversable phenotypic state where, despite antibiotic-mediated inhibition of critical
55 processes, they are able to survive[12-14]. In addition, a number of physiologic stresses increase
56 antibiotic tolerance in a population, as bacterial cell death is markedly slowed by stresses such
57 as nutrient deprivation or acidic pH[10, 11, 15, 16]. Notably, these same stresses are encountered in the
58 lysosome of an activated immune cell[17], and studies of pathogens isolated from activated
59 macrophages indeed show a strong immune-mediated increase antibiotic tolerance[9, 18]. Thus,
60 paradoxically, the immune system can actually impede bacterial eradication by antibiotics.
61
62 Antibiotic tolerance has been studied extensively in model systems such as *Escherichia coli*,
63 which has provided important insights, but also highlighted uncertainties of current models.
64 Several different regulators of antibiotic tolerance have been identified in *E. coli* including the
65 HipBA toxin-antitoxin system[19], guanosine pentaphosphate ((p)ppGpp) synthesis by RelA/SpoT
66 enzymes[20, 21], and the activity of Lon protease[20]. In each of these models, the postulated
67 mechanism is to arrest cell division and render the process targeted by antibiotics non-essential.
68 However, important questions remain unanswered. It is unclear how cells remain viable when
69 critical processes such as transcription or translation are blocked by antibiotics, as well as how
70 the process is regulated and induced by stress. Even the mechanism of cell death following
71 antibiotic exposure itself has been a matter of debate - originally antibiotics were presumed to kill
72 bacteria as a direct result of inhibition of their target molecule, such as β-lactam antibiotics
73 disrupting cell wall integrity, directly leading to mechanical cell lysis[22]. However, a number of
74 studies, largely from *E. coli*, have demonstrated that in addition to the initial target inhibition, which
75 may be bacteriostatic, bactericidal antibiotics can also cause secondary lethal ROS accumulation,
76 leading to cell death[14, 23-28].
77

78 Mycobacterial persister cells are particularly resilient, as *Mycobacterium smegmatis* (*Msmeg*) and
79 *Mycobacterium tuberculosis (Mtb)* persisters can endure many weeks of antibiotic exposure, and
80 stress-induced antibiotic tolerance develops readily[10, 14, 29]. *Mabs* is a species of rapidly-growing
81 mycobacteria, with a doubling time of ~4h in rich media[30], and while often environmental, it causes
82 opportunistic infections in patients with structural lung disease such as cystic fibrosis. It is also
83 among the most difficult of all bacterial pathogens to treat, because in addition to forming persister
84 cells, it is also intrinsically resistant to many classes of antibiotics, leaving few treatment options[5].
85 This leads to the use of antibiotics with greater toxicity to patients, and a need to use these agents
86 for prolonged periods to prevent relapse. Thus, identifying the genes that *Mabs* persister cells rely
87 on for survival, as well as the genes involved in the induction and maintenance of stress-induced
88 antibiotic tolerance might highlight pathways that could be targeted therapeutically to eliminate
89 antibiotic-tolerant cells.
90
91 Previous genetic screens have studied antibiotic responses in mycobacteria, with some
92 evaluating heritable resistance, and others investigating tolerance. Several studies of resistance
93 have successfully used either transposon mutagenesis with insertion site sequencing (Tn-Seq)
94 or CRISPR-based transcriptional repression with high-throughput sequencing of guide RNAs
95 (CRISPRi) to identify genes promoting growth in sub-inhibitory concentrations of antibiotic. These
96 studies have provided insights such as highlighting the importance of cell membrane permeability
97 as a mechanism controlling antibiotic penetration into the cytoplasm[31-33].
98
99 Persister formation has proven challenging to study, likely because the low frequency of persisters
100 leads to population bottlenecks that confound genetic analysis. Although screens in *Mtb* have been
101 conducted in macrophages and mice, and genes such as *glpK* and *cinA* identified, overall the
102 number of mutants isolated in these screens has been low[34-35]. There has been one effective in
103 vitro Tn-Seq study examining antibiotic tolerance in *Mtb* exposed to starvation and rifampin that

104 isolated over 100 mutants[27], demonstrating the feasibility of genetic screening in this context.
105 However, whether these phenotypes seen with rifampin in *Mtb* extend to other mycobacteria and
106 other antibiotics remains to be determined.
107
108 Here, we study antibiotic tolerance in *Mabs*, and describe the results of a genome-wide Tn-seq
109 screens seeking to identify the genes required for both spontaneous persister cell survival as well
110 as starvation-induced antibiotic tolerance following exposure to translation-inhibiting antibiotics.
111 We identified several discrete processes contributing to survival, and observed a prominent role
112 for ROS detoxifying factors such as the catalase-peroxidase enzyme KatG, which contributed to
113 both spontaneous persister survival and starvation-induced antibiotic tolerance. Consistent with
114 the protection conferred by KatG, we found that endogenous ROS accumulated following
115 antibiotic exposure, and that the removal of oxygen significantly impaired bacterial killing. Taken
116 together these findings support a model in mycobacteria where the lethality of translation-
117 inhibiting antibiotics is amplified by a secondary accumulation of toxic ROS, and that survival
118 requires active detoxification systems.
119
120 **RESULTS**
121 **Starvation-induced antibiotic tolerance in mycobacteria**
122 We first sought to develop conditions suitable for genetic analysis of persister cell survival and
123 stress-induced antibiotic tolerance mycobacteria. Genetic screens examining persister cell
124 physiology face two inherent obstacles. First, these cells are rare in unstressed bacterial
125 populations, and antibiotic-mediated cell death creates population bottlenecks that obscure
126 mutant phenotypes. Second, most mycobacterial populations contain spontaneous drug-resistant
127 mutants that can expand if the population is exposed to a single antibiotic. To overcome these
128 obstacles, we sought to establish large-scale, high-density culture conditions to prevent genetic
129 bottlenecks, and used multiple antibiotics to suppress spontaneous drug-resistant mutants. We

130 began by assessing the feasibility of this approach using wild-type *Msmeg.* We exposed the cells
131 to either the combination of rifampin, isoniazid, and ethambutol (RIF/INH/EMB) used to treat *Mtb*,
132 or to the combination of tigecycline and linezolid (TIG/LZD), two translation-inhibiting antibiotics
133 frequently used to treat *Mabs*[6, 36], and empirically determined the minimum inhibitory
134 concentrations (MICs) and minimum bactericidal concentrations (MBC) for each antibiotic under
135 the high-density culture conditions that would be needed for genetic analysis of persister cells.
136 Both antibiotic combinations reduced the bacterial population >1000-fold within 72h (Figure 1A).
137 We then evaluated both spontaneous persister formation and stress-induced tolerance under
138 these conditions in *Msmeg*. We compared logarithmically growing (mid-log) cultures in 7H9 rich
139 media to cultures starved for 2 days in phosphate buffered saline (PBS) prior to addition of
140 antibiotics. Consistent with expectations, we found a marked increase in antibiotic tolerance in
141 starved cultures, with a 100-fold increase in survival following TIG/LZD exposure and a 10,000-
142 fold increase following RIF/INH/EMB exposure (Figure 1A).
143
144 We next examined two species of pathogenic mycobacteria under these conditions to similarly
145 assess starvation-induced antibiotic tolerance[37-40]. We again compared cells starved in PBS to
146 logarithmically growing cells in 7H9, and found that cultures of wild-type *Mabs* (ATCC 19977) and
147 *Mtb* (Erdman) also displayed dramatic increases antibiotic tolerance in nutrient-deprived cultures
148 (Figure 1B,C). Notably, for *Mabs* and *Msmeg,* the development of tolerance required an
149 adaptation period of several days under starvation conditions, as survival was dramatically
150 impaired if cells were shifted immediately into nutrient-deficient conditions with antibiotics,
151 suggesting that a regulated process needed to be completed. Surprisingly, *Mtb* tolerance
152 developed rapidly without pre-adaptation suggesting that this organism might have additional
153 response pathways enabling more rapid adaptation.
154
155 **Identification of pathways needed for antibiotic tolerance in *Mabs***

156 We used these conditions to carry out Tn-Seq screens in *Mabs* to identify genes necessary for
157 both the survival of spontaneous persister cells and for starvation-induced antibiotic tolerance.
158 We conducted the screen using a *Mabs Himar1* Tn library comprised of ~55,000 mutations across
159 ~91,000 possible TA insertion sites covering all 4,992 non-essential *Mabs* genes in strain ATCC
160 19977[33]. To study spontaneous persister cells, cultures were maintained in continuous log-phase
161 in 7H9 rich media for 48h prior to antibiotic exposure, and then exposed to TIG/LZD for 6 days
162 (Figure 2A) a point at which spontaneous persister cells comprise the majority of the population
163 (Figure 1C). To study starvation-induced tolerance, cultures were starved in PBS for 48h prior to
164 antibiotic exposure in PBS. Following antibiotic treatment, cells were then washed and
165 resuspended in antibiotic-free liquid media to recover, and passaged 1:100 three times in
166 continuous log-phase to expand surviving cells. We then isolated genomic DNA, sequenced the
167 Tn insertion sites, and used TRANSIT software[41] to quantify the abundance of each Tn mutant
168 across different conditions to identify genes with statistically-significant differences in distribution.
169 We identified 277 *Mabs* genes required for surviving TIG/LZD exposure in rich media, 271 genes
170 required for survival during starvation and 362 genes required to survive the combined exposure
171 to antibiotics and starvation (Log_2 fold-change > 0.5 and Benjamini–Hochberg adjusted p-value
172 (p-adj.) ≤ 0.05; Figure 2B-E). Of the genes required for survival, ~60% were required in both
173 nutrient-replete and starvation states, although condition-specific determinants were also seen
174 (Figure 2F). As expected, we identified genes with already-established functions in antibiotic
175 responses, including *MAB_2752* and *MAB_2753* which are both homologs of known antibiotic
176 transporters in *Mtb,* as well as tetracycline-responsive transcription factors like *MAB_4687* and
177 *MAB_0314c* (Table S1), indicating an ability of these Tn-Seq conditions to identify physiologically
178 relevant genes known to mitigate antibiotic stress.
179
180 To identify other cellular processes necessary for survival we performed pathway enrichment
181 analysis on the set of genes identified by Tn-Seq. We used the DAVID[42] analysis tool to perform

182 systematic queries of the KEGG, GO, and Uniprot databases and identify over-represented
183 processes and pathways. Interestingly, although cells were exposed to translation-inhibiting
184 antibiotics, and no exogenous oxidative or nitrosative stress was applied, we identified a number
185 of factors needed to combat these stresses in spontaneous persister cells. This included *bfrB*
186 (bactoferritin), *ahpE* (peroxiredoxin) and *katG* (catalase/peroxidase) as well as 5 components of
187 the bacterial proteasome pathway, known to mediate resistance to nitrosative stress in *Mtb*[43]
188 (Figure 2G, Table S2). We also identified multiple members of DNA-damage response pathways
189 including *recF*, *recG*, *uvrA*, *uvrB* and *uvrC*. Examining genes required for starvation-induced
190 tolerance, a number of the same pathways were again seen, and the mutant with the greatest
191 survival defect in this context was *mntH*, a redox-regulated Mn^{2+}/Zn^{2+} transporter implicated in
192 peroxide resistance in other organisms[44-45].
193
194 To independently confirm a role in antibiotic tolerance for a set of genes from diverse pathways
195 that were identified by Tn-Seq we selected a set of genes required for survival, representing
196 several of the functional pathways identified, and used oligonucleotide-mediated recombineering
197 (ORBIT)[46] to disrupt their open reading frames. The initial genes selected were *pafA* (proteasome
198 pathway), *katG* (catalase-peroxidase), *recR* (DNA repair), *blaR* (β-lactam sensing), and
199 *MAB_1456c* (cobalamin synthesis). To control for non-specific effects of antibiotic selection during
200 the recombineering process, we created a control strain using ORBIT to target a non-coding
201 intergenic region downstream of a redundant tRNA gene (*MAB_t5030c*). We then individually
202 screened each of these mutants to determine if they displayed deficits in survival by exposing
203 cells to TIG/LZD, either in rich 7H9 media or under starvation conditions, as had been done in the
204 Tn-Seq screen. For Δ*katG* we detected clear defects in survival as soon as 3 days after antibiotic
205 exposure in either rich media or under starvation conditions, corroborating the results of our Tn-
206 Seq analysis (Figure 3A). We observed similar, albeit smaller, defects in the Δ*pafA,* Δ*MAB_1456c*,

207 and Δ*blaR,* mutants under the conditions predicted by the screen, whereas we saw no defect in
208 the Δ*recR* mutant (Figure 3B-E). We also noted that several mutants displayed delays in growth
209 recovery after antibiotic removal at times before survival defects were noted (Figure 3
210 Supplement). To further confirm the role of *katG* and *pafA,* and exclude off-target effects of
211 recombineering, we performed genetic complementation analysis by restoring a wild-type copy of
212 each gene into the respective Δ*pafA* and Δ*katG* mutants. In each case, we integrated a single
213 copy of the wild-type gene, under the control of its endogenous promoter, into the genome at the
214 L5 *attB* site (hereafter *pafA*+*, katG*+ strains), and constructed isogenic control strains with an
215 empty vector integrated at the same site (hereafter *pafA*-*, katG*- strains). We confirmed
216 expression of the re-introduced copy of each gene by RT-qPCR in the *pafA*+, and *katG*+ strains,
217 and found expression within roughly 2-fold of endogenous wild-type levels (Figure 4A,D). We then
218 challenged these strains with TIG/LZD as before. In rich media, where the Δ*katG* mutants have a
219 moderate survival defect, the *katG*+ strain had roughly a 50-fold increase in viable cells relative
220 to the *katG*- strain. We then exposed cells to antibiotics under starvation conditions, where the
221 Δ*katG* mutant phenotype is more severe. Under these conditions the *katG*- cells succumbed
222 rapidly between 3d and 10d after antibiotic exposure, with a 1,000-fold decrease in viable cells
223 relative to control cells, whereas the *katG*+ strain showed a near-complete restoration of antibiotic
224 tolerance (Figure 4B). We analogously examined complementation of Δ*pafA* mutants, and
225 although the phenotype of the Δ*pafA* mutant is less severe overall than a Δ*katG* mutant, we saw
226 a similar restoration of survival in *pafA*+ cells relative to *pafA*- cells (Figure 4E). We next evaluated
227 whether the *pafA*-, and *katG*- strains were overall more sensitive to the growth inhibitory effects
228 of TIG/LZD, or whether they had specific defects in survival above the mean bactericidal
229 concentration. We performed MIC determination for TIG and LZD individually for each strain,
230 comparing the *katG*+/*katG*- and *pafA*+/*pafA*- strains. We found that that the MICs for each of
231 these strains were unchanged, demonstrating that these mutants were not more readily inhibited

232 by these antibiotics. Instead, they have more rapid kinetics of cell death at bactericidal
233 concentrations, consistent with a specific defect in antibiotic tolerance, and supporting a model
234 whereby an initial growth-arresting inhibition of the direct antibiotic target can be uncoupled
235 mechanistically from a distinct cell-death step (Figure 4C,F), as has been seen with other
236 antibiotic classes[26].
237
238 **Reactive oxygen contributes to antibiotic lethality in *Mabs***
239 We next investigated the role of KatG and reactive oxygen in antibiotic tolerance more broadly.
240 We began by assessing whether KatG conferred protection from other antibiotics with diverse
241 mechanisms of action, selecting antibiotics that are used clinically for mycobacterial infections.
242 Because *katG*- mutants showed the greatest defects in starvation-induced tolerance, we analyzed
243 survival of *katG*+ and *katG*- strains in starvation-adapted cultures exposed to a panel of different
244 antibiotics. Because both TIG and LZD both act by inhibiting translation, we began by exposing
245 cells to either TIG or LZD alone. As expected, the degree of bacterial killing was significantly less
246 with either agent alone than when they are added in combination. Upon exposure to either of
247 these antibiotics the *katG*- cells died more rapidly than *katG*+ cells, though we note that the final
248 proportion of persister cells in the population was unchanged in *katG*- cells (Figure 5A). When
249 we exposed cells to rifabutin, an RNA polymerase inhibitor, we saw a similar effect, with a 100-
250 fold loss of viability in *katG*- cells relative to the *katG*+ cells (Figure 5B). In contrast, when we
251 exposed cultures to either levofloxacin (topoisomerase inhibitor) or cefoxitin (β-lactam inhibitor of
252 peptidoglycan cross-linking), *katG* had little to no effect on cell viability (Figure 5C-D). Thus, the
253 role of KatG is context-dependent, suggesting that some antibiotics generate oxidative stress that
254 can be ameliorated by KatG while others do not.
255
256 The identification of *katG* as essential for cells to survive exposure to TIG/LZD suggests that ROS
257 are present and causing damage. Although TIG/LZD are translation inhibitors that do not directly

258 generate ROS we evaluated whether they might nonetheless be triggering ROS accumulation as
259 a secondary effect. We examined ROS levels in control *Mabs* using the ROS indicator dye
260 cellROX, that is retained in cells when it becomes oxidized[47]. At baseline, during log-phase growth
261 in rich media < 2% of cells had ROS accumulation (Figure 5E). We saw a moderate increase in
262 ROS accumulation in starved cultures, with roughly 7% of the population cellROX+. However,
263 when cells were exposed to antibiotics we saw a dramatic accumulation of ROS, with 57% of cells
264 becoming cellROX+ when exposed to TIG/LZD in rich media and 33% of PBS-starved cells
265 becoming cellROX+ when exposed to TIG/LZD. Taken together, these data indicate that
266 translation inhibition does indeed have important downstream effects on cellular redox balance,
267 with ROS accumulation that could be contributing to the lethal effects of antibiotics.
268
269 We next tested whether ROS were contributing to cell death by reducing ROS production and
270 assessing the impact on cell viability. A well-established system for studying hypoxia in
271 mycobacteria is the Wayne Model of gradual-onset hypoxia, whereby low-density cultures are
272 inoculated in sealed vessels with minimal headspace. As the culture slowly grows, the soluble
273 oxygen is consumed, resulting in the slow onset of hypoxia over several days, a process that can
274 be monitored by the decolorization of Methylene Blue dye in the media[48]. Under aerobic conditions
275 in rich media, we observed the expected rapid killing of *Mabs* over the first 5 days with the
276 combination of TIG/LZD, with more rapid loss of viability in KatG- cells. However, under hypoxic
277 conditions, where ROS production is suppressed, we saw much slower bacterial killing.
278 Importantly, under hypoxic conditions *katG*- cells no longer had a survival defect relative to *katG*+
279 cells, supporting the hypothesis that translation-inhibiting antibiotics also cause secondary
280 accumulation of lethal ROS in antibiotic-treated cells that need to be detoxified by KatG (Figure
281 5F).
282

283 We also evaluated whether other methods of alleviating ROS damage might enhance survival.
284 The iron chelator 2,2'-dipyridyl has been shown in other contexts to reduce ROS-mediated
285 damage by suppressing the reaction of H_20_2 with Fe^{2+} that generates highly oxidizing hydroxyl
286 radicals (Fenton reaction), and which has been shown to mitigate oxidative damage in other
287 bacteria following antibiotic exposure[23, 26, 49]. As seen in other bacteria, we find that in *Mabs*, 2,2'-
288 dipyridy does indeed improve bacterial survival following exposure to bactericidal translation
289 inhibitors, further supporting a role in ROS in cell death following translation inhibition (Figure 5G).
290 We also assessed whether free radical scavengers like thiourea and 2,2,6,6-
291 tetramethylpiperidine-1-oxyl (TEMPO) ameliorated antibiotic toxicity, although similar antioxidants
292 had previously been shown in *Mtb* to increase respiration and paradoxically to increase ROS
293 generation[27]. When we treated *Mabs* simultaneously with TIG/LZD in combination with either
294 thiourea or TEMPO we did not observe a restoration of antibiotic tolerance, and, similar to
295 observations in *Mtb,* actually observed increased bacterial cell death (Figure 5 Supplement).
296

297 **Incomplete penetrance of *katG* phenotype among *Mabs* strains**

298 To test whether ROS accumulation was an effect occurring more broadly across different *Mabs*
299 strains we obtained two clinical strains, exposed them to TIG/LZD in 7H9 media, and measured
300 ROS accumulation with cellROX as above. We found that similar to ATCC 19977, both clinical
301 *Mabs* strains had elevated ROS levels following translation inhibition (Figure 6A), suggesting that
302 this is a conserved process in *Mabs*. Next, we tested the role of KatG in these *Mabs* clinical
303 strains. We used ORBIT to disrupt the *katG* locus, and evaluated the ability of these Δ*katG* clinical
304 strains to survive exposure to TIG/LZD under both stressed and un-stressed conditions. Unlike
305 ROS accumulation, where the responses across strains were consistent, we saw a variable
306 dependency on *katG*. Clinical strain-1 behaved differently overall, with no appreciable starvation-
307 induced antibiotic tolerance, and no contribution of *katG* to survival. In contrast, for clinical strain-
308 2, *katG* contributed significantly to starvation-induced antibiotic tolerance, behaving similarly to

309 the ATCC 19977 reference strain. However, unlike the reference strain, *katG* was not required for
310 survival of clinical strain-2 when exposed to antibiotics in 7H9 media (Figure 6B). Thus, although
311 antibiotic-induced ROS accumulation was observed across all three *Mabs* strains, the Δ*katG*
312 phenotype displays incomplete penetrance, suggesting that in some *Mabs* strains alternative
313 pathways exist that are able to compensate the loss of *katG.*
314
315 In summary, the results of these studies point to an important effect of ROS in amplifying the
316 lethality of transcription and translation-inhibiting antibiotics in *Mabs*. Through genetic analysis we
317 identified a number of ROS detoxification factors, including KatG, as necessary for survival in this
318 context. This suggested that antibiotics induced an oxidative state in cells, and direct
319 measurement of ROS following antibiotic exposure indicated that this was indeed the case.
320 Further supporting the toxic effects of ROS in this context, we found that removal of oxygen both
321 slowed bacterial killing and rendered KatG dispensable. Taken together these results suggest that
322 in *Mabs* antibiotic lethality is accelerated by ROS accumulation, and that survival requires active
323 detoxification systems.
324
325 **DISCUSSION:**
326 **Pathways necessary for antibiotic tolerance in *Mabs.***
327 The phenomenon of antibiotic tolerance has been recognized for decades, and has been
328 observed in a broad array of bacterial species, but without a uniform underlying mechanism -
329 suggesting that different pathways may play roles in different physiologic contexts. For example,
330 the pathways identified in one bacterial species may not contribute to tolerance in another. In
331 addition to *E. coli, relA* plays a role in tolerance in *Pseudomonas aeruginosa*[53]*, Staphylococcus*
332 *aureus*[54], and *Mtb*[55]. However, its role is not universal. Deletion of *relA* had no effect on antibiotic
333 tolerance in *Msmeg*[56], and in our Tn-Seq analysis, *Mabs relA* Tn mutants had no survival defect.
334 However, a prior study of the *Mabs relA* mutant demonstrated that this strain still synthesizes

335 (p)ppGpp[57], suggesting potential genetic redundancy. Even within a single species there can be
336 differences in the critical survival mechanisms depending on the context. In *E. coli,* RelA
337 contributes to persister viability following exposure to β-lactams, but not quinolones[53], and in our
338 study we find KatG to be essential for tolerance to transcription and translation inhibitors but not
339 to β-lactams or quinolones.
340
341 **Mechanisms of antibiotic lethality**
342 Our findings strongly support the idea that ROS can be a significant contributor to antibiotic lethality
343 in *Mabs*, and contribute to the growing evidence that this is conserved across mycobacteria. In *Mabs,*
344 *Mtb* and *Msmeg,* other groups have also observed reduced antibiotic-mediated killing in hypoxic
345 conditions[25, 37]. In addition, in *Mtb*, exposure to rifampin also generates ROS[19,60], and *katG*
346 contributes to survival in rifampin-treated cells[26].
347
348 Exactly how transcription or translation blockade leads to increased ROS levels is also not known.
349 In principle, any of several derangements could lead to ROS accumulation. One of the major
350 sources of cellular ROS is oxidative phosphorylation, as hydrogen peroxide and superoxide are
351 natural byproducts. Thus, increased ROS generation by oxidative phosphorylation is an attractive
352 hypothesis. Alternatively, particularly under starvation conditions, it is possible that antioxidants
353 and ROS scavengers may become depleted, creating a more oxidizing environment. Our Tn-Seq
354 analysis provides additional insight on this. We noted a small class of Tn mutants that were
355 paradoxically protected from antibiotic lethality (Figure 2B). Prominent among this class of
356 mutants were several independent components of the NADH dehydrogenase complex. Also
357 known as Complex I of the electron transport chain, it is one of the key entry points for electrons
358 into the oxidative phosphorylation pathway. The observation that mutants lacking this complex
359 are protected suggests that decreasing flux through oxidative phosphorylation, with a concomitant

360 decrease in ROS generation, may enhance survival during antibiotic exposure. A mechanistic
361 understanding of how blockade of either transcription or translation leads to deranged oxygen
362 utilization is an unresolved question that will require further study.
363
364 ROS accumulation is not universal following exposure to bactericidal antibiotics. While antibiotic-
365 induced ROS is well-documented, under some conditions, such as higher concentrations of
366 antibiotic, multiple studies have also observed antibiotic lethality without ROS accumulation[23, 58-
367 61]. Similarly, prior studies have found that under certain conditions, *E. coli* mutants lacking
368 catalase have defects in antibiotic tolerance[62-64], whereas under other conditions they do not[23, 65].
369 In *Mabs* the role of *katG* was also not uniform, as it had no impact on survival following exposure
370 to levofloxacin or cefoxitin. Additional studies will be needed to determine whether levofloxacin
371 and cefoxitin kill without generating ROS, or whether ROS is generated but effectively detoxified
372 in the absence of *katG.* This latter possibility is suggested by our findings in *Mabs* clinical strains.
373 While we saw ROS accumulation in both strains after TIG/LZD exposure, the role of *katG* was
374 variable between the strains. This suggests that compensatory pathways likely exist and that in
375 *Mabs* they can overcome the loss of *katG.*
376
377 **Therapeutic implications**
378 *Mabs* infections are particularly challenging to treat, with relapse rates over 50%[3]. Our results
379 highlight several bacterial processes, such as the bacterial proteasome and ROS detoxification,
380 that might be targeted therapeutically to reduce the survival of antibiotic tolerant bacteria in
381 patients with *Mabs* infection. Agents targeting these process might not have any intrinsic
382 antimicrobial activity alone, but might act to disrupt the unique physiology required to survive
383 antibiotics. This would represent a new therapeutic class of “persistence inhibitors” that might act
384 synergistically with traditional antibiotics to eliminate the subpopulation of cells that would

385 otherwise remain viable despite prolonged antibiotic treatment in patients with *Mabs* and other
386 chronic infections[6, 27].
387
388 **Limitations**
389 Tn-Seq has inherent drawbacks, including an inability to identify mutants in essential genes, or in
390 cases of genetic redundancy. Thus, there are likely genes needed for antibiotic tolerance in *Mabs*
391 that were not identified in this study. In addition, we studied the response to a single class of
392 antibiotic, focusing on the translation inhibitors often used to treat *Mabs* infections, and we studied
393 only spontaneous persister cells and starvation-induced antibiotic tolerance. It is likely that
394 examining other antibiotics, with different mechanisms of action, or different stresses that induce
395 tolerance would identify additional genes contributing to survival and would allow identification of
396 core pathways that might be shared in differing physiologic contexts of antibiotic and stress[25, 27].
398
399 **MATERIALS AND METHODS**
400 **Key Reagent Table**

Reagent	**Source/Reference**	**Identifier**
***Mabs* ATCC 19977**	ATCC	19977
***Msmeg* MC2 155**	ATCC	700084
***Mtb* Erdman**	ATCC	35801
***Mabs* clinical strains**	Sacramento Department of Public Health	NA
pkm444	Addgene	108319
pkm496	Addgene	109301
pmv306	Ref. [66]	
Middlebrook 7H9	BD	271310

Middlebrook 7H10	BD	262710
Glycerol	Invitrogen	15514011
Tween-80	Fisher	BP338-500
Middlebrook OADC	BD	212351
DPBS (-Ca/Mg)	Gibco	14190144
Tyloxapol	Sigma Aldrich	T8761
Methylene blue	Sigma Aldrich	28514
Tigecycline	Chem Impex	29737
Linezolid	Chem Impex	29723
Levofloxacin	Sigma Aldrich	28266
Cefoxitin	Chem Impex	1490
Rifabutin	Cayman Chemical	16468
Rifampin	Sigma Aldrich	R7382
Isoniazid	Supelco	I3377
Ethambutol	Thermo Scientific	J6069506
DMSO	Sigma Aldrich	D2650
Trizol	Invitrogen	15596018
0.1mm zirconia beads	Biospec	11079101z
PureLink RNA Mini Kit	Invitrogen	12183025
Kanamycin	VWR	75856-686
Zeocin	Invivogen	ANTZN1P
Glycine	Fisher Bioreagents	BP381
Sucrose	Sigma Aldrich	S1888
Anhydrotetracycline	Cayman Chemical	10009542
cellROX green	Invitrogen	C10444

Paraformaldehyde	Sigma Aldrich	P6148
DAPI	Sigma Aldrich	D9542
DNAseI	New England Biolabs	M0303
Maxima H minus reverse transcriptase	Thermo Scientific	EP0752
Taq Polymerase	New England Biolabs	M0273
EvaGreen	Biotium	31019
Bipyridyl	Sigma Aldrich	D216305
Thiourea	Sigma Aldrich	T7875
4-Hydroxy-TEMPO	Simga Aldrich	176141

Bacterial strains and culture conditions:

Mabs ATCC 19977, clinical *Mabs* strains and *Msmeg* (MC2 155) were grown in BD Middlebrook 7H9 media (liquid) or 7H10 media (solid) supplemented with 0.5% glycerol (Sigma) and 0.2% Tween-80 (Fisher) but without any OADC supplementation except for transformations. Sacramento clinical isolates were obtained from the Sacramento County Department of Public Health Mycobacteriology Laboratory. Confirmation of clinical isolates as *Mabs* was performed by amplifying the 16s rRNA locus and Sanger sequencing (maybe reference new data table?). *Mtb* (Erdman) was grown in 7H9 (liquid) or 7H10 (solid) supplemented with 0.5% glycerol, 0.1% Tween-80, and 10% OADC (BD). All cultures were grown at 37°C with gentle shaking. Except for specific hypoxia conditions, all liquid cultures were grown with 90% container headspace or using a gas permeable cap to ensure culture oxygenation. PBS starvation was achieved by washing OD0.5-1.0 *Mabs* 1X in DPBS (-Ca/Mg, Gibco) and resuspending in DPBS at OD=1, supplemented with 0.1% tyloxapol (Sigma).

416 *Mabs* antibiotic experiments:

417 For PBS starvation experiments, stocks of *Mabs* were grown for 48 hours in 7H9 passaging
418 continuously in log phase, then PBS starved or passaged in log phase for an additional 48h. Log
419 phase or PBS starved *Mabs* were then resuspended in antibiotic containing media at OD1.0. For
420 experiments with hypoxia, *Mabs* in mid-log aerobic growth was adjusted to OD0.001 in media
421 with 1.5μg/ml methylene blue and added to a rubber septum sealed glass vial with 50%
422 headspace. Methylene blue discoloration was observed at 3d and antibiotics were added at 5d.
423 For thiourea and TEMPO experiments, these were added to the cultures at the time of antibiotic
424 administration. For bipyridyl experiments, 62.5μM bipyridyl was added to the cultures 2h prior to
425 antibiotic administration. We empirically determined the half-life of each antibiotic in 7H9 media
426 at 37-deg and for those with half-lives shorter than the experiment, supplemented cultures to with
427 additional antibiotic to maintain the concentration of active antibiotic. Antibiotics were used at the
428 following concentrations: tigecycline (Chem-Impex) at 10μg/ml (8 fold above MIC, re-administered
429 every 3 days), linezolid (Chem-Impex) at 100μg/ml (20 fold above MIC), levofloxacin (Sigma) at
430 40μg/ml (8 fold above MIC), cefoxitin (Chem Impex) at 80μg/ml (8 fold above MIC, re-
431 administered every 3 days), and rifabutin (Cayman) at 40μg/ml (4 fold above MIC). After antibiotic
432 administration, colony forming units over time were measured by plating on 7H10 solid media.
433 For experiments where growth recovery time in liquid media was quantified, 100μl of sample was
434 removed at d6 after antibiotic administration and washed 2X in antibiotic-free media. The samples
435 were resuspended in 5ml of antibiotic free media, and OD620 measurements were taken with a
436 FilterMax F3 plate reader (Molecular Devices) until maximum cell density (OD of ~5.0) was
437 reached.

438

439 *Msmeg* antibiotic experiments:

440 Individual colonies were picked and grown for 48 hours in log phase before being PBS starved or
441 passaged in log phase for 48h. Log phase or PBS starved *Msmeg* were then resuspended in

442 antibiotic containing media at OD1.0. Antibiotics were used at the following concentrations:
443 tigecycline (Chem-Impex) at 1.25μg/ml (8 fold above MIC, re-administered every 3 days), linezolid
444 (Chem-Impex) at 2.5μg/ml (8 fold above MIC), rifampin (Sigma) at 32μg/ml (8 fold above MIC, re-
445 administered every 6 days), isoniazid (Sigma) at 32μg/ml (8 fold above MIC, re-administered
446 every 6 days), and ethambutol (Thermo) at 4μg/ml (8 fold above MIC, re-administered every 3
447 days). After antibiotic administration, colony forming units over time were measured.
448
449 *Mtb* antibiotic experiments:
450 Freezer stocks of *Mtb* were thawed and grown for 5-7 days in log phase before being starved for
451 14d or longer. Non-starved control *Mtb* were thawed such that they were also grown for 5-7 days
452 in log phase before experimental use. Log phase or PBS starved *Mtb* was then resuspended in
453 antibiotic containing media and adjusted to OD1.0. Antibiotics were used at the following
454 concentrations: rifampin (Sigma) at 0.1μg/ml (4 fold above MIC, re-administered every 6 days),
455 isoniazid (Sigma) at 0.1μg/ml (4 fold above MIC, re-administered every 6 days), and ethambutol
456 (Thermo) at 8μg/ml (4 fold above MIC, re-administered every 6 days). After antibiotic
457 administration, colony forming units over time were measured.
458
459 Transposon insertion sequencing:
460 The construction of this *Himar1* transposon Tn library has been described previously[33]. Screening
461 was performed by growing a freezer stock of the library for 2.5 days in log phase before 48-hour
462 PBS starvation or further continuous log-phase growth. Samples were then resuspended in media
463 containing either tigecycline/linezolid or an equal volume of DMSO solvent and incubated for 6
464 days, with a re-administration of tigecycline or matching DMSO on day 3. Cultures were aerated
465 by culturing in a vented cap bottle with gentle agitation at 40 revolutions per minute throughout
466 the experiment. The samples were then washed 2X in antibiotic free liquid media, resuspended
467 in antibiotic free liquid media (10X the original culture volume), and grown until OD0.5-1.0.

468 Subsequently, the samples underwent three more rounds of 100-fold passaging in liquid media
469 to amplify surviving bacteria before the samples were collected in Trizol (Invitrogen). A sample
470 taken at the time of the commencement of PBS starvation was collected in Trizol and used as the
471 input control. Three independent trials of this experiment were submitted to the UC Davis DNA
472 Technologies Core, where Tn insertion site flanking sequences were amplified as described
473 previously[33] and sequenced on sequenced on an Illumina AVITI. Sequence reads were mapped
474 to the ATCC 19977 genome and analyzed using TRANSIT software with the following parameters:
475 0% of N/C termini ignored, 10,000 samples, TTR normalization, LOESS correction, include sites
476 with all zeros, site restricted resampling. Genes with significant changes were defined as those
477 with adjusted p-value (p-adj.) <0.05 and $\log_2$ fold change >0.5. P-adj. was calculated using the
478 Benjamini-Hochberg correction.
479
480 Pathway enrichment analysis
481 To improve gene annotation, *Mabs* orthologs to *Mtb* genes were identified. *Mabs* genes were first
482 converted into protein sequences using Mycobrowser, and protein sequences were then used to
483 perform reciprocal BLASTp searches. *Mabs* genes and *Mtb* genes that mapped to each other
484 using independent one-way BLASTp searches with a maximum e-value cutoff of 0.1 were
485 considered orthologs. For pathway analysis, gene lists (*Mtb* orthologs) were then imported into
486 the DAVID knowledgebase[42] and pathway enrichment analysis performed for Gene Ontology
487 biological process, Uniprot keyword and KEGG databases with statistical analysis Fisher's exact
488 test and nominal p-value reported.
489
490 Gene deletion and complementation:
491 Knockout strains were generated using ORBITT[48]. Briefly, *Mabs* was transformed with the
492 kanamycin-resistant ORBIT recombineering plasmid pkm444. 20ml *Mabs* at OD0.5-1.0 was
493 washed 2X in 10% glycerol and resuspended in 200ul 10% glycerol. 500ng plasmid was added

494 and electroporated at 2.5kV in 0.2cm cuvettes. The bacteria were allowed to recover overnight
495 before plating on 150µg/ml kanamycin plates. Clones were selected and regrown in liquid media
496 supplemented with 150µg/ml kanamycin and 10% OADC (BD) to OD0.5-1.0. For recombineering,
497 the pkm444-*Mabs* was grown to mid-log, then diluted to OD0.1 and 200mM glycine (Fisher) was
498 added to the media. 16 hours later, 500mM sucrose (Sigma) and 500ng/ml anhydrotetracycline
499 (Cayman) were added and incubated for an additional 4 hours. Subsequently, the *Mabs* was
500 washed 2X in ice cold 10% glycerol + 500mM sucrose. 200ul of 10X concentrated *Mabs* was then
501 electroporated with 600ng of the zeocin-R ORBIT payload pkm496 plasmid and 2µg of targeting
502 oligonucleotide (Table S3) at 2.5kV in 0.2cm cuvettes. The *Mabs* was then allowed to recover
503 overnight in liquid media with 10% OADC and 500ng/ml anhydrotetracycline before being plated
504 on 150µg/ml zeocin plates. Mutants were then selected and screened for gene deletion by PCR
505 amplification and Sanger sequencing. For genetic complementation, the endogenous loci
506 including promoter and terminator sequences were amplified by PCR and cloned into the EcoRV
507 site of pmv306 with kanamycin resistance[66]. In the case of *katG,* the upstream gene *furA* was
508 also included in the complementation construct to achieve optimal *katG* expression.
509
510 MIC determination
511 Two-fold serial dilutions of antibiotics were prepared in a 96 well plate in 100ul volume. 100ul of
512 2X bacteria were added (for *Mabs*: used a final OD of 0.001, *Msmeg*: OD0.001, *Mtb*: OD0.01),
513 making a final volume of 200µl. The plates were incubated until there was visible growth in the no
514 antibiotic control well. At this time, the bacteria were transferred to a new plate with 20µl of 40%
515 paraformaldehyde and OD620 measurements were taken with a FilterMax F3 plate reader
516 (Molecular Devices).
517
518 Flow cytometry

519 OD1 Mab was stained with cellROX green (Invitrogen) at a final concentration of 5μM for 1hr at
520 37C. The cells were then washed in PBS and resuspended in PBS with 4% paraformaldehyde
521 and 5μg/ml DAPI (Sigma). The samples were run on a LSRII flow cytometer (BD). Fluorophores
522 were excited with the 405nm (DAPI) and 488nm (cellROX) lasers. Detection was performed using
523 the 450/50 (505LP) filter for DAPI and a 525/50 (555LP) filter for cellROX. Data were analyzed
524 with FlowJo software (BD).
525
526 DNA/RNA Purification:
527 Samples were resuspended in 5 volumes of Trizol and were bead beat with 0.1mm zirconia beads
528 (Biospec) 6x2min at 4°C in a Mini-Beadbeater-16 (Biospec). Chloroform was added and RNA in
529 the aqueous phase removed. For DNA isolation, a second RNA extraction was performed with
530 0.8M guanidine thiocyanate and 0.5M guanidine hydrochloride, 60mM Acetate pH 5.2, 1mM
531 EDTA. DNA was then isolated with back-extraction buffer (4M Guanidine Thiocyanate, 50mM
532 Sodium Citrate, 1M Tris base (without pH adjustment ~pH 11) and DNA purified using a PureLink
533 RNA Mini Kit (Invitrogen).
534
535 RT-qPCR
536 RNA was purified using PureLink RNA Mini Kit per manufacturer's instructions. The samples were
537 DNAseI (NEB) treated for 15min/37°C before stopping the reaction by adding 3.5mM EDTA and
538 heating for 10min/75°C. cDNA was synthesized from 500ng total RNA using random hexamers
539 and Maxima H minus reverse transcriptase (Thermo). No reverse-transcription controls were also
540 included and used to confirm the lack of genomic DNA-driven amplification. qPCR reactions used
541 Taq polymerase (NEB) and EvaGreen (Biotium) and were run on Biorad CFX Opus 96 Real-Time
542 PCR System. Melt curves were included for each sample to confirm uniform amplicon identity
543 between samples. Gene-specific amplification was quantified by comparison to a standard curve

544 generated from 3-fold serial dilutions of a control sample, then normalized to 16S rRNA within
545 each sample.
546
547 **FIGURE LEGENDS**
548 **Figure 1. Starvation induces antibiotic tolerance in diverse mycobacteria.** (A) *Msmeg,* (B)
549 *Mtb* or (C) *Mabs* were grown in 7H9 rich media or starved in PBS prior to the addition of antibiotics
550 and surviving colony forming units (CFU) enumerated. For the rapidly-growing mycobacteria,
551 *Msmeg* and *Mabs,* cells were allowed to adapt for 48h prior to antibiotics, for slow-growing *Mtb,*
552 cells were allowed to adapt for 14-21d prior to antibiotics. Samples without pre-adaptation were
553 washed and placed directly into PBS with antibiotics. Antibiotic concentrations were: *Msmeg* -
554 Isoniazid (INH) 32μg/ml (8 x MIC), rifampin (RIF) 32μg/ml (8 x MIC), ethambutol (EMB) 4μg/ml (8
555 x MIC), tigecycline (TIG) 1.25μg/ml (8 x MIC), linezolid (LZD) 2.5μg/ml (8 x MIC). *Mtb* – RIF
556 0.1μg/ml (4 x MIC), INH at 0.1μg/ml (4 x MIC), EMB at 8μg/ml (4 x MIC). *Mabs* – TIG 10μg/ml (8
557 x MIC), LZD 100μg/ml (20 x MIC). Antibiotics with half-lives shorter than the duration of
558 experiment were re-added at the following intervals: TIG, EMB every 3d; RIF, INH every 6d. Error
559 bars represent SEM, statistical significance is calculated at each time point using student's t test.
560 ****: $p<0.0001$, ***: $p<0.001$, **: $p<0.01$, *: $p<0.05$, ns: $p>0.05$. Data are combined from 3
561 independent experiments.
562
563 **Figure 2. Tn-Seq identifies genes required for antibiotic tolerance in *Mabs*.** (A) Experimental
564 design. (B-E) Tn-Seq analysis showing relative abundance of individual genes under the indicted
565 conditions. Genes depleted relative to the input population have negative values. All cultures were
566 fully aerated throughout the experiment and cultures without antibiotics received and equal
567 volume of DMSO. For (B-D) gene abundance in the indicated condition is measured relative the
568 input log-phase population. In (E) an additional comparison is made for PBS with antibiotics
569 relative to the PBS condition. Genes with significant decreases in abundance are shown in color

570 (p-adj. < 0.05 and log_2 fold-change > 0.5) using the Benjamini–Hochberg adjustment for multiple
571 hypothesis testing. (F) Number of genes essential in each condition relative to the input
572 population. (G) Pathway enrichment analysis of the essential genes in each condition using the
573 DAVID knowledgebase (p <0.05). Screens were run as 3 independent experiments and the
574 combined results analyzed. Antibiotic conditions were as described above.
575
576 **Figure 3. Validation of Tn-Seq results.** (A-E) Homologous recombination was used to delete
577 the indicated genes, or to generate a control strain targeting a distant intergenic region distal to
578 the non-essential tRNA gene *MAB_t5030c*. Each strain was either grown in 7H9 rich media or
579 starved in PBS for 48 prior to the addition of antibiotics as indicated. The conditions tested here
580 correspond to the conditions in the Tn-Seq analysis where a phenotype was observed. Data from
581 additional conditions are in Figure 3 Supplemental. Comparisons in panels A-C are made to the
582 same control strain but plotted independently for clarity. Error bars represent SEM, statistical
583 significance is calculated at each time point using student's t test. ****: p<0.0001, ***: p<0.001, **:
584 p<0.01, *: p<0.05, ns: p>0.05. Antibiotics were added as described above. Data are
585 representative from 4 independent experiments.
586
587 **Figure 4. Complementation analysis *katG* and *pafA* mutants confirms their role in antibiotic**
588 **tolerance.** (A) RT-qPCR analysis of *katG* expression in *katG- (Δ katG::pmv306), katG+*
589 *(Δ katG::pmv306 katG),* and control strain (ORBIT intergenic*::pmv306*). (B) CFU over time for
590 *katG+/katG-* strains. (C) MICs for *katG+/katG-* strains. (D) Expression of *pafA in pafA-*
591 *(Δ pafA::pmv306), pafA+* (*pafA::pmv306 pafA*) and control strain. (E) CFU over time for
592 *pafA+/pafA-* strains. (F) MICs for *pafA+/pafA-* strains. Antibiotic concentrations in (A-B, D-E) are
593 as described above. Error bars represent SEM, statistical significance is calculated at each time
594 point using student's t test between *katG+/katG-* strains in (B) and between *pafA+/pafA-* strains

595 in (E). ****: p<0.0001, ***: p<0.001, **: p<0.01, *: p<0.05, ns: p>0.05. Antibiotics were added as
596 described above.
597
598 **Figure 5. ROS-mediated toxicity following antibiotic exposure.** (A-D) Analysis of *katG+/katG-*
599 cells challenged with different antibiotics. Cells were starved in PBS for 48h and then exposed to
600 the indicated antibiotic. (E) Flow cytometry of control cells exposed to TIG/LZD (4h in 7H9 media
601 or 72h in PBS) and then stained with DAPI and the ROS-sensitive dye cellROX green; percentage
602 cellROX-positive cells are indicated. (F) Survival over time for aerated and hypoxic cultures of
603 *Mabs* after exposure to TIG/LZD. (G) Survival over time for bipyridyl treated cells after exposure
604 to TIG/LZD. Error bars represent SEM, statistical significance is calculated at each time point
605 using student's t test. ****: p<0.0001, ***: p<0.001, **: p<0.01, *: p<0.05, ns: p>0.05. (A-D, F)
606 display combined data from 3 independent experiments. (E, G) are representative data from 3
607 independent experiments.
608
609 **Figure 6. Consistent antibiotic-induced ROS production but variable protection by KatG**
610 **among different *Mabs* strains.** (A) The indicated strains of *Mabs* were cultured in 7H9 media,
611 exposed to TIG/LZD for 4h and then analyzed by cellROX staining. (B) CFU over time following
612 TIG/LZD exposure. Error bars represent SEM, statistical significance is calculated at each time
613 point using student's t test. ****: p<0.0001, ***: p<0.001, **: p<0.01, *: p<0.05, ns: p>0.05.
614 Combined data from 4 independent experiments are shown for persister survival experiments.
615 Representative data from 2 independent experiments are shown for flow cytometry experiments.
616 Antibiotics were added as described above.
617
618 **Figure 3 Supplement. Additional analysis of mutants.** (A) *blaR* or (B) *recR* mutants were
619 examined under conditions where Tn-Seq did not predict a phenotype. Cells were starved in PBS
620 for 48h prior to treatment with TIG/LZD or DMSO as described in Figure 3. (C) Growth recovery

621 of mutants after antibiotic exposure. After 6 d of TIG/LZD exposure cells were washed twice in
622 antibiotic free media and inoculated into 7H9 media. Growth was monitored by OD 600 of the
623 culture. Error bars represent SEM, statistical significance is calculated at each time point using
624 student's t test. ****: $p<0.0001$, ***: $p<0.001$, **: $p<0.01$, *: $p<0.05$, ns: $p>0.05$. (A-B) are
625 representative data from 4 independent experiments (C) is representative data from 2
626 independent experiments.
627
628 **Figure 5 Supplement. Effect of ROS scavengers.** *ΔkatG* cells were starved in PBS for 48h then
629 treated with TIG/LZD and the indicated concentration of (A) thiourea or (B) TEMPO and surviving
630 CFU over time were measured. Representative data from 2 independent experiments are shown.
631
632
633
634 **Table S1. Tn-Seq results**
635 **Table S2. DAVID functional pathway analysis**
636 **Table S3. Oligonucleotide sequences**
637 **Table S4. 16s sequencing data of clinical strains**
638
639 **ACKNOWLEDGEMENTS**
640 We would like to thank Nick Campbell-Kruger for his technical insights on identifying *Mabs/Mtb*
641 orthologs, Jonathan Van Dyke for his assistance with flow cytometry analysis, Emily Kumimoto
642 and Siranoosh Ashtari for their assistance with Tn-Seq library preparation and sequencing, and
643 Jessie Li and Bradley Jenner for their assistance with Tn-seq bioinformatics. We would also like
644 to thank Caroline Dominic at the Sacramento County Department of Public Health for providing
645 clinical isolates of *Mabs* for analysis.
646

FUNDING

Pew Biomedical Fellowship BHP

NIH RO1 1R01AI144149 BHP

NIH R01 1R01AI143722 SAS

NIH Shared Instrumentation Grant 1S10OD010786-01 DNA Technologies and Expression Analysis Core, UC Davis Genome Center

NCI Cancer Center Support Grant P30CA093373 Flow Cytometry Shared Resource, UC Davis

CONFLICTS OF INTEREST

BHP and SAS serve on the scientific advisory board of X-Biotics Therapeutics.

REFERENCES

1. Stevens, D.L., A.L. Bisno, H.F. Chambers, E.P. Dellinger, E.J. Goldstein, S.L. Gorbach, J.V. Hirschmann, S.L. Kaplan, J.G. Montoya, and J.C. Wade, *Practice guidelines for the diagnosis and management of skin and soft tissue infections: 2014 update by the Infectious Diseases Society of America.* Clin Infect Dis, 2014. **59**(2): p. e10-52.
2. Metersky, M.L. and A.C. Kalil, *Management of ventilator-associated pneumonia: guidelines.* Clinics in chest medicine, 2018. **39**(4): p. 797-808.
3. Griffith, D.E. and C.L. Daley, *Treatment of Mycobacterium abscessus Pulmonary Disease.* CHEST, 2022. **161**(1): p. 64-75.
4. Nahid, P., S.E. Dorman, N. Alipanah, P.M. Barry, J.L. Brozek, A. Cattamanchi, L.H. Chaisson, R.E. Chaisson, C.L. Daley, and M. Grzemska, *Official American thoracic society/centers for disease control and prevention/infectious diseases society of America clinical practice guidelines: treatment of drug-susceptible tuberculosis.* Clinical infectious diseases, 2016. **63**(7): p. e147-e195.

673 5. Griffith, D.E., T. Aksamit, B.A. Brown-Elliott, A. Catanzaro, C. Daley, F. Gordin, S.M.
674 Holland, R. Horsburgh, G. Huitt, and M.F. Iademarco, *An official ATS/IDSA statement:*
675 *diagnosis, treatment, and prevention of nontuberculous mycobacterial diseases.*
676 American journal of respiratory and critical care medicine, 2007. **175**(4): p. 367-416.
677 6. Meylan, S., I.W. Andrews, and J.J. Collins, *Targeting Antibiotic Tolerance, Pathogen by*
678 *Pathogen.* Cell, 2018. **172**(6): p. 1228-1238.
679 7. Namugenyi, S.B., A.M. Aagesen, S.R. Elliott, and A.D. Tischler, *Mycobacterium*
680 *tuberculosis PhoY Proteins Promote Persister Formation by Mediating Pst/SenX3-*
681 *RegX3 Phosphate Sensing.* mBio, 2017. **8**(4): p. e00494-17.
682 8. Liu, Y., S. Tan, L. Huang, R.B. Abramovitch, K.H. Rohde, M.D. Zimmerman, C. Chen, V.
683 Dartois, B.C. VanderVen, and D.G. Russell, *Immune activation of the host cell induces*
684 *drug tolerance in Mycobacterium tuberculosis both in vitro and in vivo.* Journal of
685 Experimental Medicine, 2016. **213**(5): p. 809-825.
686 9. Gold, B. and C. Nathan, *Targeting Phenotypically Tolerant Mycobacterium tuberculosis.*
687 Microbiol Spectr, 2017. **5**(1).
688 10. Bigger, J.J.T.L., *Treatment of staphylococcal infections with penicillin by intermittent*
689 *sterilisation.* 1944. **244**(6320): p. 497-500.
690 11. Ronneau, S., P.W.S. Hill, and S. Helaine, *Antibiotic persistence and tolerance: not just*
691 *one and the same.* Current opinion in microbiology, 2021. **64**: p. 76-81.
692 12. Dhar, N. and J.D. McKinney, *Microbial phenotypic heterogeneity and antibiotic tolerance.*
693 Current opinion in microbiology, 2007. **10**(1): p. 30-38.
694 13. Grant, S.S., B.B. Kaufmann, N.S. Chand, N. Haseley, and D.T. Hung, *Eradication of*
695 *bacterial persisters with antibiotic-generated hydroxyl radicals.* Proceedings of the
696 National Academy of Sciences, 2012. **109**(30): p. 12147-12152.
697 14. Baker, J.J. and R.B. Abramovitch, *Genetic and metabolic regulation of Mycobacterium*
698 *tuberculosis acid growth arrest.* Scientific Reports, 2018. **8**(1).

699 15. Saito, K., T. Warrier, S. Somersan-Karakaya, L. Kaminski, J. Mi, X. Jiang, S. Park, K.
700 Shigyo, B. Gold, and J. Roberts, *Rifamycin action on RNA polymerase in antibiotic-*
701 *tolerant Mycobacterium tuberculosis results in differentially detectable populations.*
702 Proceedings of the National Academy of Sciences, 2017. **114**(24): p. E4832-E4840.
703 16. Hipolito, V.E.B., E. Ospina-Escobar, and R.J. Botelho, *Lysosome remodelling and*
704 *adaptation during phagocyte activation.* Cell Microbiol, 2018. **20**(4).
705 17. Sukumar, N., S. Tan, B.B. Aldridge, and D.G. Russell, *Exploitation of Mycobacterium*
706 *tuberculosis reporter strains to probe the impact of vaccination at sites of infection.* PLoS
707 Pathog, 2014. **10**(9): p. e1004394.
708 18. Schumacher, M.A., K.M. Piro, W. Xu, S. Hansen, K. Lewis, and R.G. Brennan, *Molecular*
709 *Mechanisms of HipA-Mediated Multidrug Tolerance and Its Neutralization by HipB.*
710 Science, 2009. **323**(5912): p. 396-401.
711 19. Harms, A., C. Fino, A. Sørensen Michael, S. Semsey, and K. Gerdes, *Prophages and*
712 *Growth Dynamics Confound Experimental Results with Antibiotic-Tolerant Persister*
713 *Cells.* mBio, 2017. **8**(6): p. 10.1128/mbio.01964-17.
714 20. Korch, S.B., T.A. Henderson, and T.M. Hill, *Characterization of the hipA7 allele of*
715 *Escherichia coli and evidence that high persistence is governed by (p)ppGpp synthesis.*
716 Mol Microbiol, 2003. **50**(4): p. 1199-213.
717 21. Wong, F., S. Wilson, R. Helbig, S. Hegde, O. Aftenieva, H. Zheng, C. Liu, T. Pilizota, E.C.
718 Garner, A. Amir, and L.D. Renner, *Understanding Beta-Lactam-Induced Lysis at the*
719 *Single-Cell Level.* Frontiers in Microbiology, 2021. **12**.
720 22. Kohanski, M.A., D.J. Dwyer, B. Hayete, C.A. Lawrence, and J.J. Collins, *A common*
721 *mechanism of cellular death induced by bactericidal antibiotics.* Cell, 2007. **130**(5): p.
722 797-810.
723 23. Dwyer, D.J., P.A. Belenky, J.H. Yang, I.C. MacDonald, J.D. Martell, N. Takahashi, C.T.Y.
724 Chan, M.A. Lobritz, D. Braff, E.G. Schwarz, J.D. Ye, M. Pati, M. Vercruysse, P.S. Ralifo,

K.R. Allison, A.S. Khalil, A.Y. Ting, G.C. Walker, and J.J. Collins, *Antibiotics induce redox-related physiological alterations as part of their lethality.* Proceedings of the National Academy of Sciences, 2014. **111**(20): p. E2100-E2109.

24. Zeng, J., Y. Hong, N. Zhao, Q. Liu, W. Zhu, L. Xiao, W. Wang, M. Chen, S. Hong, L. Wu, Y. Xue, D. Wang, J. Niu, K. Drlica, and X. Zhao, *A broadly applicable, stress-mediated bacterial death pathway regulated by the phosphotransferase system (PTS) and the cAMP-Crp cascade.* Proc Natl Acad Sci U S A, 2022. **119**(23): p. e2118566119.

25. Shee, S., S. Singh, A. Tripathi, C. Thakur, T.A. Kumar, M. Das, V. Yadav, S. Kohli, R.S. Rajmani, N. Chandra, H. Chakrapani, K. Drlica, and A. Singh, *Moxifloxacin-Mediated Killing of Mycobacterium tuberculosis Involves Respiratory Downshift, Reductive Stress, and Accumulation of Reactive Oxygen Species.* Antimicrob Agents Chemother, 2022. **66**(9): p. e0059222.

26. Saito, K., S. Mishra, T. Warrier, N. Cicchetti, J. Mi, E. Weber, X. Jiang, J. Roberts, A. Gouzy, E. Kaplan, C.D. Brown, B. Gold, and C. Nathan, *Oxidative damage and delayed replication allow viable Mycobacterium tuberculosis to go undetected.* Sci Transl Med, 2021. **13**(621): p. eabg2612.

27. Vilchèze, C., T. Hartman, B. Weinrick, P. Jain, T.R. Weisbrod, L.W. Leung, J.S. Freundlich, and W.R. Jacobs, Jr., *Enhanced respiration prevents drug tolerance and drug resistance in Mycobacterium tuberculosis.* Proc Natl Acad Sci U S A, 2017. **114**(17): p. 4495-4500.

28. Saito, K., S. Mishra, T. Warrier, N. Cicchetti, J. Mi, E. Weber, X. Jiang, J. Roberts, A. Gouzy, E. Kaplan, C.D. Brown, B. Gold, and C. Nathan, *Oxidative damage and delayed replication allow viable Mycobacterium tuberculosis to go undetected.* Science Translational Medicine, 2021. **13**(621): p. eabg2612.

29. Dorman, S.E., P. Nahid, E.V. Kurbatova, P.P. Phillips, K. Bryant, K.E. Dooley, M. Engle, S.V. Goldberg, H.T. Phan, and J. Hakim, *Four-month rifapentine regimens with or without*

751 *moxifloxacin for tuberculosis.* New England Journal of Medicine, 2021. **384**(18): p. 1705-
752 1718.
753 30. Hunt-Serracin Augusto, C., J. Parks Brian, J. Boll, and C. Boutte Cara, *Mycobacterium*
754 *abscessus Cells Have Altered Antibiotic Tolerance and Surface Glycolipids in Artificial*
755 *Cystic Fibrosis Sputum Medium.* Antimicrobial Agents and Chemotherapy, 2019. **63**(7):
756 p. 10.1128/aac.02488-18.
757 31. Li, S., N.C. Poulton, J.S. Chang, Z.A. Azadian, M.A. DeJesus, N. Ruecker, M.D.
758 Zimmerman, K.A. Eckartt, B. Bosch, C.A. Engelhart, D.F. Sullivan, M. Gengenbacher,
759 V.A. Dartois, D. Schnappinger, and J.M. Rock, *CRISPRi chemical genetics and*
760 *comparative genomics identify genes mediating drug potency in Mycobacterium*
761 *tuberculosis.* Nature microbiology, 2022. **7**(6): p. 766-779.
762 32. Carey, A.F., J.M. Rock, I.V. Krieger, M.R. Chase, M. Fernandez-Suarez, S. Gagneux,
763 J.C. Sacchettini, T.R. Ioerger, and S.M. Fortune, *TnSeq of Mycobacterium tuberculosis*
764 *clinical isolates reveals strain-specific antibiotic liabilities.* PLoS pathogens, 2018. **14**(3):
765 p. e1006939.
766 33. Rodriguez, R., N. Campbell-Kruger, J. Gonzalez Camba, J. Berude, R. Fetterman, and
767 S. Stanley, *MarR-Dependent Transcriptional Regulation of mmpSL5 Induces*
768 *Ethionamide Resistance in Mycobacterium abscessus.* Antimicrobial Agents and
769 Chemotherapy, 2023. **67**(4): p. e01350-22.
770 34. Kreutzfeldt, K.M., R.S. Jansen, T.E. Hartman, A. Gouzy, R. Wang, I.V. Krieger, M.D.
771 Zimmerman, M. Gengenbacher, J.P. Sarathy, M. Xie, V. Dartois, J.C. Sacchettini, K.Y.
772 Rhee, D. Schnappinger, and S. Ehrt, *CinA mediates multidrug tolerance in*
773 *Mycobacterium tuberculosis.* Nat Commun, 2022. **13**(1): p. 2203.
774 35. Bellerose, M.M., S.-H. Baek, C.-C. Huang, C.E. Moss, E.-I. Koh, M.K. Proulx, C.M.
775 Smith, R.E. Baker, J.S. Lee, S. Eum, S.J. Shin, S.-N. Cho, M. Murray, and C.M. Sassetti,

Common Variants in the Glycerol Kinase Gene Reduce Tuberculosis Drug Efficacy. mBio, 2019. **10**(4): p. e00663-19.

36. Kumar, K., C.L. Daley, D.E. Griffith, and M.R. Loebinger, *Management of Mycobacterium avium complex and Mycobacterium abscessus pulmonary disease: therapeutic advances and emerging treatments.* European respiratory review, 2022. **31**(163).

37. Yam, Y.K., N. Alvarez, M.L. Go, and T. Dick, *Extreme Drug Tolerance of Mycobacterium abscessus "Persisters".* Front Microbiol, 2020. **11**: p. 359.

38. Berube, B.J., L. Castro, D. Russell, Y. Ovechkina, and T. Parish, *Novel Screen to Assess Bactericidal Activity of Compounds Against Non-replicating Mycobacterium abscessus.* Front Microbiol, 2018. **9**: p. 2417.

39. Lee, J., N. Ammerman, A. Agarwal, M. Naji, S.Y. Li, and E. Nuermberger, *Differential In Vitro Activities of Individual Drugs and Bedaquiline-Rifabutin Combinations against Actively Multiplying and Nutrient-Starved Mycobacterium abscessus.* Antimicrob Agents Chemother, 2021. **65**(2).

40. Betts, J.C., P.T. Lukey, L.C. Robb, R.A. McAdam, and K. Duncan, *Evaluation of a nutrient starvation model of Mycobacterium tuberculosis persistence by gene and protein expression profiling.* Molecular Microbiology, 2002. **43**(3): p. 717-731.

41. DeJesus, M.A., C. Ambadipudi, R. Baker, C. Sassetti, and T.R. Ioerger, *TRANSIT-a software tool for Himar1 TnSeq analysis.* PLoS computational biology, 2015. **11**(10): p. e1004401.

42. Huang da, W., B.T. Sherman, and R.A. Lempicki, *Systematic and integrative analysis of large gene lists using DAVID bioinformatics resources.* Nat Protoc, 2009. **4**(1): p. 44-57.

43. Darwin, K.H., S. Ehrt, J.-C. Gutierrez-Ramos, N. Weich, and C.F. Nathan, *The proteasome of Mycobacterium tuberculosis is required for resistance to nitric oxide.* Science, 2003. **302**(5652): p. 1963-1966.

801 44. Shi, H., R. Zhang, L. Lan, Z. Chen, and J. Kan, *Zinc mediates resuscitation of lactic acid-*
802 *injured Escherichia coli by relieving oxidative stress.* Journal of Applied Microbiology,
803 2019. **127**(6): p. 1741-1750.
804 45. Hohle, T.H. and M.R. O'Brian, *The mntH gene encodes the major Mn(2+) transporter in*
805 *Bradyrhizobium japonicum and is regulated by manganese via the Fur protein.* Mol
806 Microbiol, 2009. **72**(2): p. 399-409.
807 46. Jones, J.G. and G.A. Morrison, *The bacteriostatic actions of tetracycline and*
808 *oxytetracycline.* J Pharm Pharmacol, 1962. **14**: p. 808-24.
809 47. Brock, T.D., *CHLORAMPHENICOL.* Bacteriol Rev, 1961. **25**(1): p. 32-48.
810 48. Murphy, K.C., S.J. Nelson, S. Nambi, K. Papavinasasundaram, C.E. Baer, and C.M.
811 Sassetti, *ORBIT: a new paradigm for genetic engineering of mycobacterial*
812 *chromosomes.* mBio, 2018. **9**(6): p. e01467-18.
813 49. McBee, M.E., Y.H. Chionh, M.L. Sharaf, P. Ho, M.W.L. Cai, and P.C. Dedon, *Production*
814 *of superoxide in bacteria is stress- and cell state-dependent: A gating-optimized flow*
815 *cytometry method that minimizes ROS measurement artifacts with fluorescent dyes.*
816 Frontiers in Microbiology, 2017. **8**(MAR).
817 50. Wayne, L.G. and L.G. Hayes, *An In Vitro Model for Sequential Study of Shiftdown of*
818 *Mycobacterium tuberculosis through Two Stages of Nonreplicating Persistence.* Infection
819 and Immunity, 1996. **64**(6): p. 2062-2069.
820 51. Winterbourn, C.C., *Toxicity of iron and hydrogen peroxide: the Fenton reaction.* Toxicol
821 Lett, 1995. **82-83**: p. 969-74.
822 52. Imlay, J.A., S.M. Chin, and S. Linn, *Toxic DNA damage by hydrogen peroxide through*
823 *the Fenton reaction in vivo and in vitro.* Science, 1988. **240**(4852): p. 640-2.
824 53. Viducic, D., T. Ono, K. Murakami, H. Susilowati, S. Kayama, K. Hirota, and Y. Miyake,
825 *Functional analysis of spoT, relA and dksA genes on quinolone tolerance in*

826 *Pseudomonas aeruginosa under nongrowing condition.* Microbiol Immunol, 2006. **50**(4):
827 p. 349-57.
828 54. Geiger, T., B. Kästle, F.L. Gratani, C. Goerke, and C. Wolz, *Two small (p)ppGpp*
829 *synthases in Staphylococcus aureus mediate tolerance against cell envelope stress*
830 *conditions.* J Bacteriol, 2014. **196**(4): p. 894-902.
831 55. Dutta, N.K., L.G. Klinkenberg, M.J. Vazquez, D. Segura-Carro, G. Colmenarejo, F.
832 Ramon, B. Rodriguez-Miquel, L. Mata-Cantero, E. Porras-De Francisco, Y.M. Chuang,
833 H. Rubin, J.J. Lee, H. Eoh, J.S. Bader, E. Perez-Herran, A. Mendoza-Losana, and P.C.
834 Karakousis, *Inhibiting the stringent response blocks Mycobacterium tuberculosis entry*
835 *into quiescence and reduces persistence.* Sci Adv, 2019. **5**(3): p. eaav2104.
836 56. Bhaskar, A., C. De Piano, E. Gelman, J.D. McKinney, and N. Dhar, *Elucidating the role*
837 *of (p) ppGpp in mycobacterial persistence against antibiotics.* IUBMB life, 2018. **70**(9): p.
838 836-844.
839 57. Hunt-Serracín, A.C., M.I. Kazi, J.M. Boll, and C.C. Boutte, *In Mycobacterium abscessus,*
840 *the Stringent Factor Rel Regulates Metabolism but Is Not the Only (p)ppGpp Synthase.*
841 J Bacteriol, 2022. **204**(2): p. e0043421.
842 58. Imlay, J.A., *Diagnosing oxidative stress in bacteria: not as easy as you might think.* Curr
843 Opin Microbiol, 2015. **24**: p. 124-31.
844 59. Keren, I., S. Minami, E. Rubin, and K. Lewis, *Characterization and transcriptome*
845 *analysis of Mycobacterium tuberculosis persisters.* mBio, 2011. **2**(3): p. e00100-11.
846 60. Ezraty, B., A. Vergnes, M. Banzhaf, Y. Duverger, A. Huguenot, A.R. Brochado, S.Y. Su, L.
847 Espinosa, L. Loiseau, B. Py, A. Typas, and F. Barras, *Fe-S cluster biosynthesis controls*
848 *uptake of aminoglycosides in a ROS-less death pathway.* Science, 2013. **340**(6140): p.
849 1583-7.
850 61. Malik, M., S. Hussain, and K. Drlica, *Effect of anaerobic growth on quinolone lethality*
851 *with Escherichia coli.* Antimicrob Agents Chemother, 2007. **51**(1): p. 28-34.

852 62. Goswami, M., S.H. Mangoli, and N. Jawali, *Involvement of Reactive Oxygen Species in*
853 *the Action of Ciprofloxacin against Escherichia coli.* Antimicrobial Agents and
854 Chemotherapy, 2006. **50**(3): p. 949-954.
855 63. Wang, X. and X. Zhao, *Contribution of oxidative damage to antimicrobial lethality.*
856 Antimicrob Agents Chemother, 2009. **53**(4): p. 1395-402.
857 64. Hong, Y., Q. Li, Q. Gao, J. Xie, H. Huang, K. Drlica, and X. Zhao, *Reactive oxygen*
858 *species play a dominant role in all pathways of rapid quinolone-mediated killing.* J
859 Antimicrob Chemother, 2020. **75**(3): p. 576-585.
860 65. Liu, Y. and J.A. Imlay, *Cell death from antibiotics without the involvement of reactive*
861 *oxygen species.* Science, 2013. **339**(6124): p. 1210-3.
862 66. Snapper, S.B., L. Lugosi, A. Jekkel, R.E. Melton, T. Kieser, B.R. Bloom, and W.R.
863 Jacobs, Jr., *Lysogeny and transformation in mycobacteria: stable expression of foreign*
864 *genes.* Proc Natl Acad Sci U S A, 1988. **85**(18): p. 6987-91.

865

866

FIGURE 1

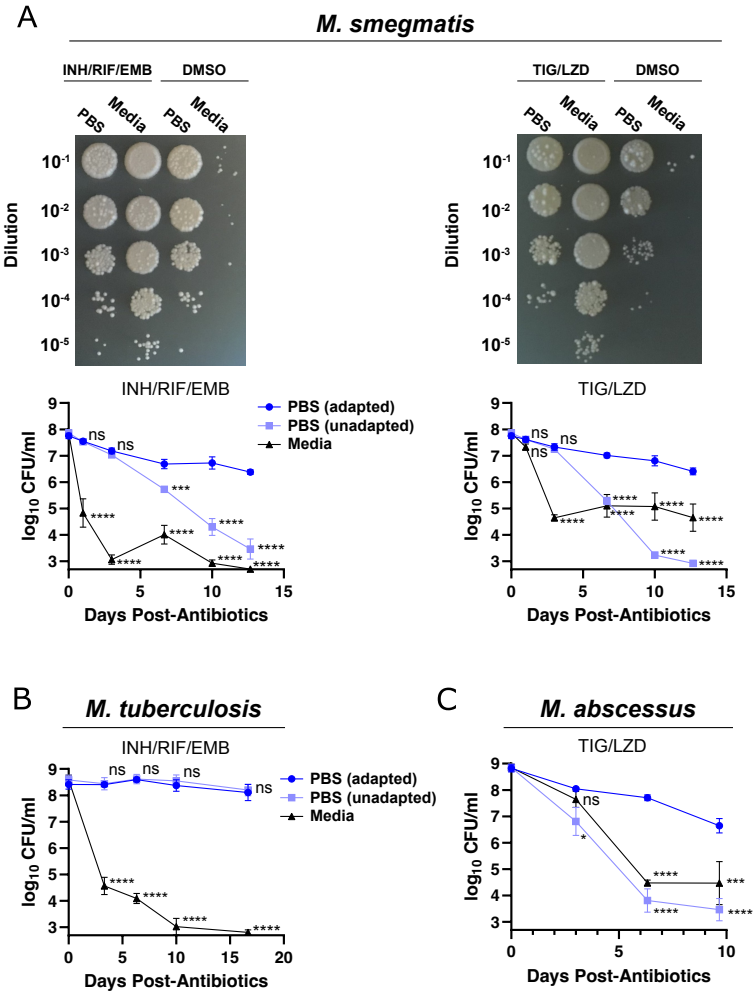
A
M. smegmatis
INH/RIF/EMB
DMSO
TIG/LZD
DMSO
PBS
Media
PBS
Media
Dilution
10-1
10-2
10-3
10-4
10-5
INH/RIF/EMB
TIG/LZD
PBS (adapted)
PBS (unadapted)
Media
log10 CFU/ml
Days Post-Antibiotics
ns
***
****

B
M. tuberculosis
INH/RIF/EMB
PBS (adapted)
PBS (unadapted)
Media
log10 CFU/ml
Days Post-Antibiotics
ns
****

C
M. abscessus
TIG/LZD
log10 CFU/ml
Days Post-Antibiotics
ns
*
***
****

FIGURE 2

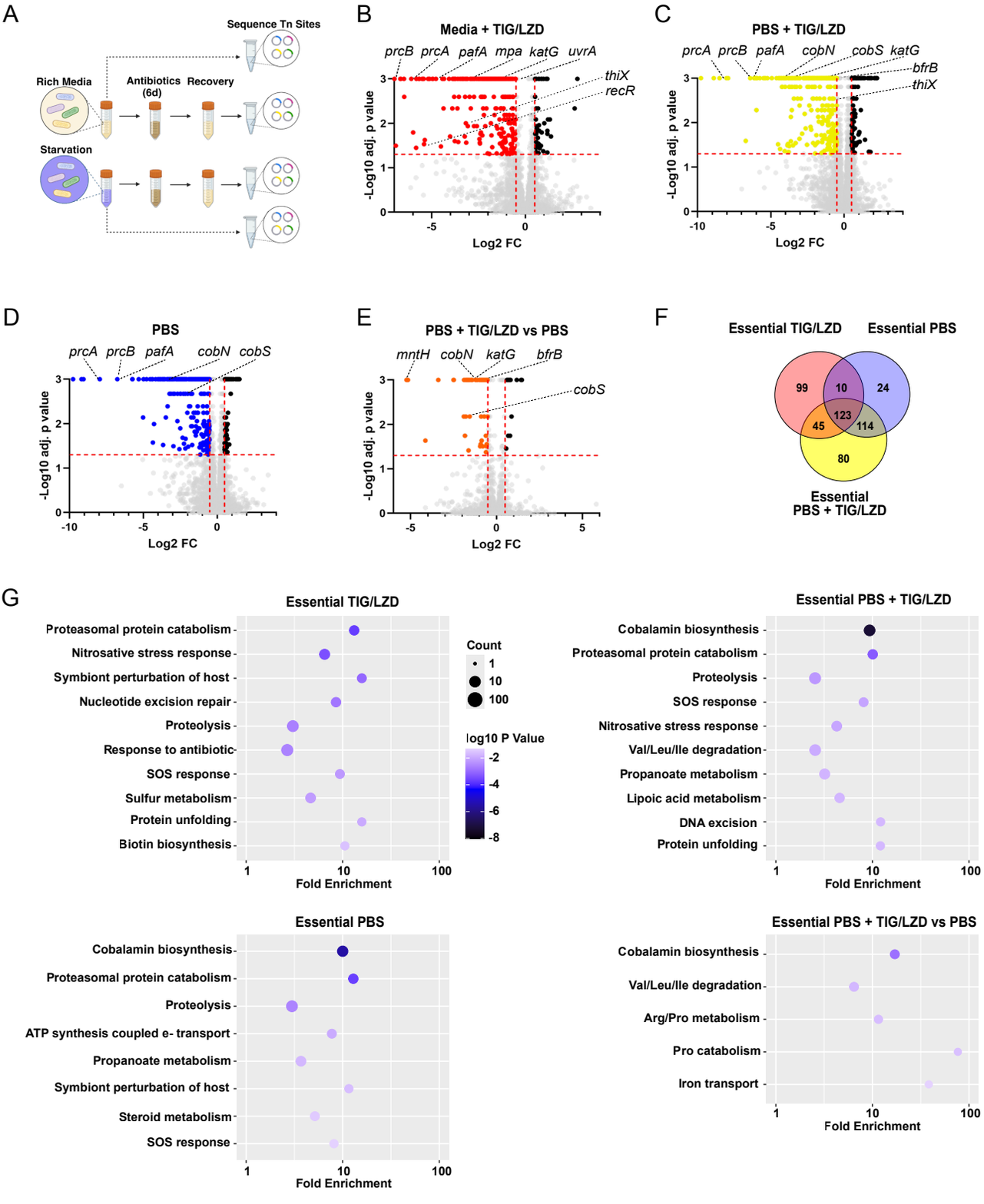
A
Sequence Tn Sites
Rich Media
Antibiotics (6d)
Recovery
Starvation
B
Media + TIG/LZD
prcB prcA pafA mpa katG uvrA
thiX
recR
-Log10 adj. p value
Log2 FC
C
PBS + TIG/LZD
prcA prcB pafA cobN cobS katG
bfrB
thiX
-Log10 adj. p value
Log2 FC
D
PBS
prcA prcB pafA cobN cobS
-Log10 adj. p value
Log2 FC
E
PBS + TIG/LZD vs PBS
mntH cobN katG bfrB
cobS
-Log10 adj. p value
Log2 FC
F
Essential TIG/LZD
Essential PBS
99
10
24
123
45
114
80
Essential PBS + TIG/LZD
G
Essential TIG/LZD
Proteasomal protein catabolism
Nitrosative stress response
Symbiont perturbation of host
Nucleotide excision repair
Proteolysis
Response to antibiotic
SOS response
Sulfur metabolism
Protein unfolding
Biotin biosynthesis
Fold Enrichment
Count
1
10
100
log10 P Value
-2
-4
-6
-8
Essential PBS + TIG/LZD
Cobalamin biosynthesis
Proteasomal protein catabolism
Proteolysis
SOS response
Nitrosative stress response
Val/Leu/Ile degradation
Propanoate metabolism
Lipoic acid metabolism
DNA excision
Protein unfolding
Fold Enrichment
Essential PBS
Cobalamin biosynthesis
Proteasomal protein catabolism
Proteolysis
ATP synthesis coupled e- transport
Propanoate metabolism
Symbiont perturbation of host
Steroid metabolism
SOS response
Fold Enrichment
Essential PBS + TIG/LZD vs PBS
Cobalamin biosynthesis
Val/Leu/Ile degradation
Arg/Pro metabolism
Pro catabolism
Iron transport
Fold Enrichment

FIGURE 3

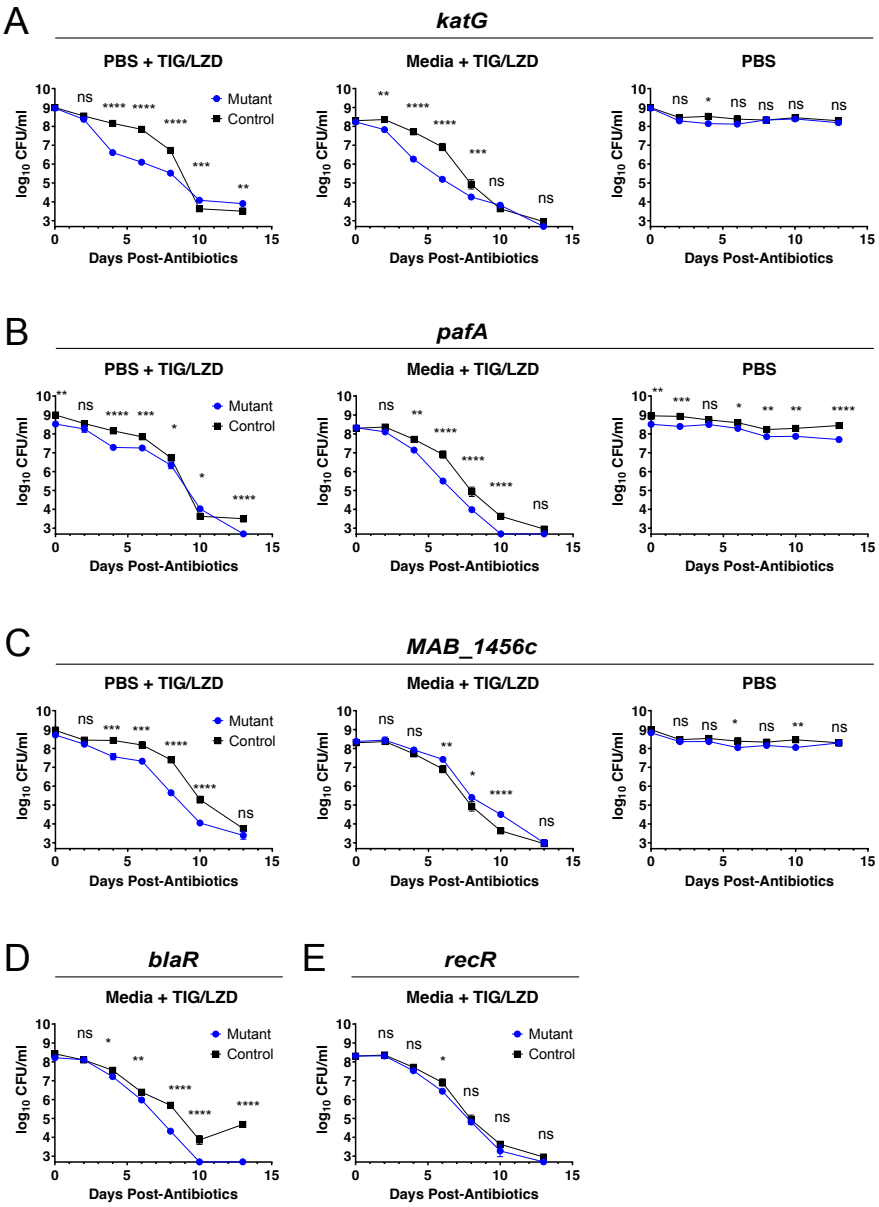
A
katG
PBS + TIG/LZD
Media + TIG/LZD
PBS
Mutant
Control
log10 CFU/ml
Days Post-Antibiotics
B
pafA
C
MAB_1456c
D
blaR
E
recR

FIGURE 4

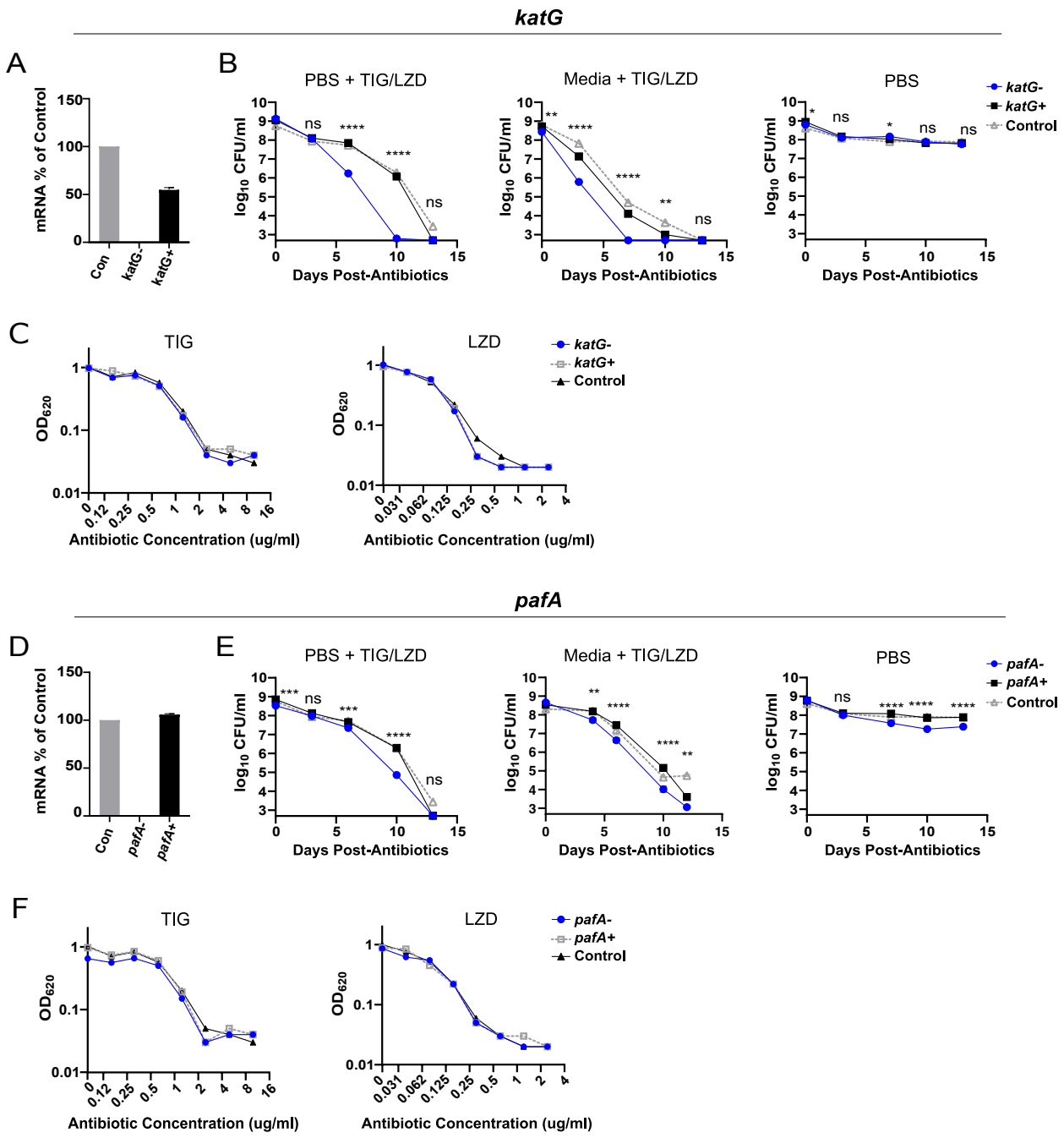
katG
A
mRNA % of Control
Con
katG-
katG+
B
PBS + TIG/LZD
Media + TIG/LZD
PBS
log10 CFU/ml
Days Post-Antibiotics
katG-
katG+
Control
C
TIG
LZD
OD620
Antibiotic Concentration (ug/ml)
pafA
D
mRNA % of Control
Con
pafA-
pafA+
E
PBS + TIG/LZD
Media + TIG/LZD
PBS
log10 CFU/ml
Days Post-Antibiotics
pafA-
pafA+
Control
F
TIG
LZD
OD620
Antibiotic Concentration (ug/ml)

FIGURE 5

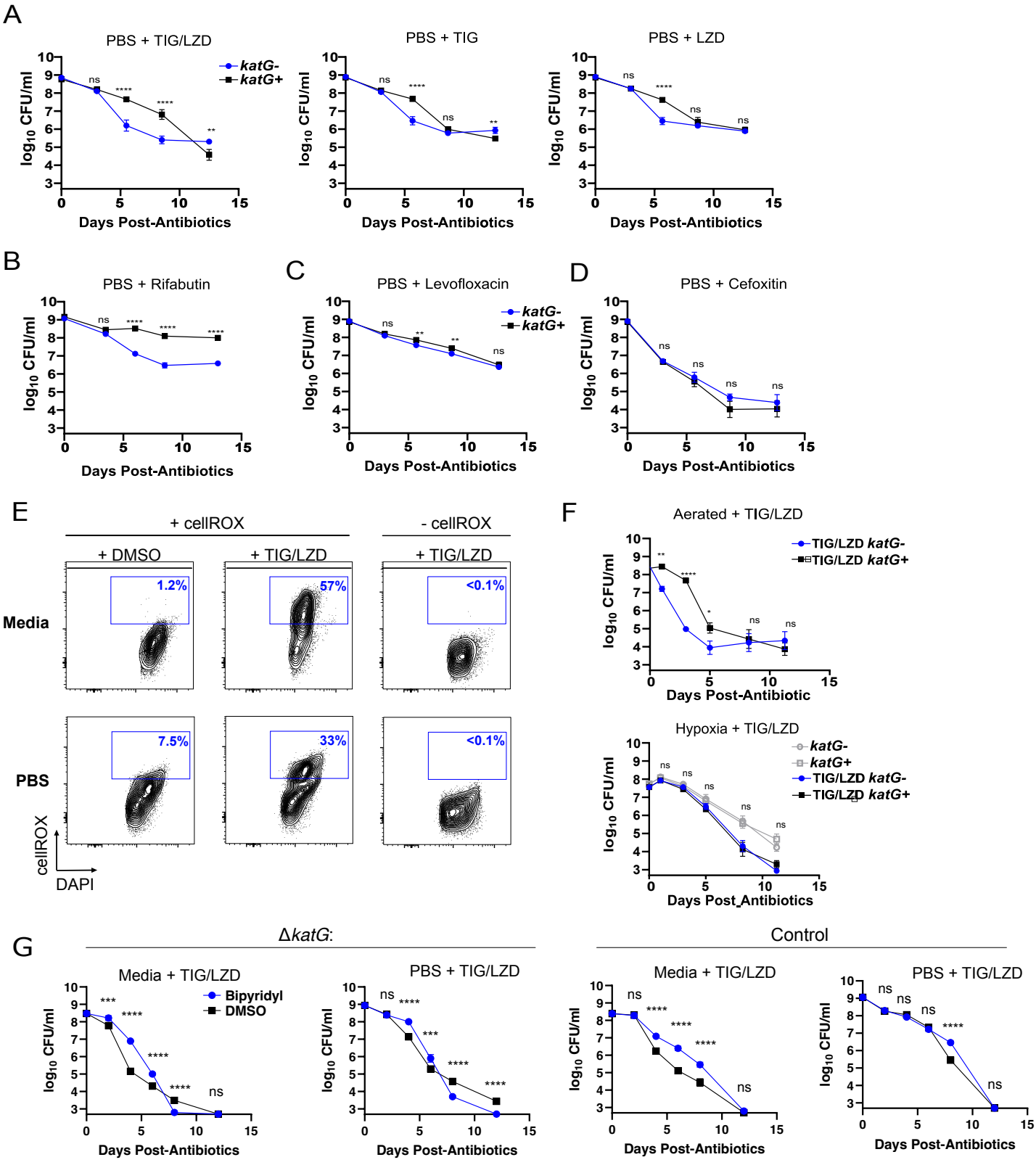
A
PBS + TIG/LZD
PBS + TIG
PBS + LZD
katG-
katG+
log10 CFU/ml
Days Post-Antibiotics
B
PBS + Rifabutin
C
PBS + Levofloxacin
D
PBS + Cefoxitin
E
+ cellROX
- cellROX
+ DMSO
+ TIG/LZD
Media
PBS
1.2%
57%
<0.1%
7.5%
33%
<0.1%
cellROX
DAPI
F
Aerated + TIG/LZD
TIG/LZD katG-
TIG/LZD katG+
Days Post-Antibiotic
Hypoxia + TIG/LZD
Days Post_Antibiotics
G
ΔkatG:
Control
Media + TIG/LZD
PBS + TIG/LZD
Bipyridyl
DMSO

FIGURE 6

A

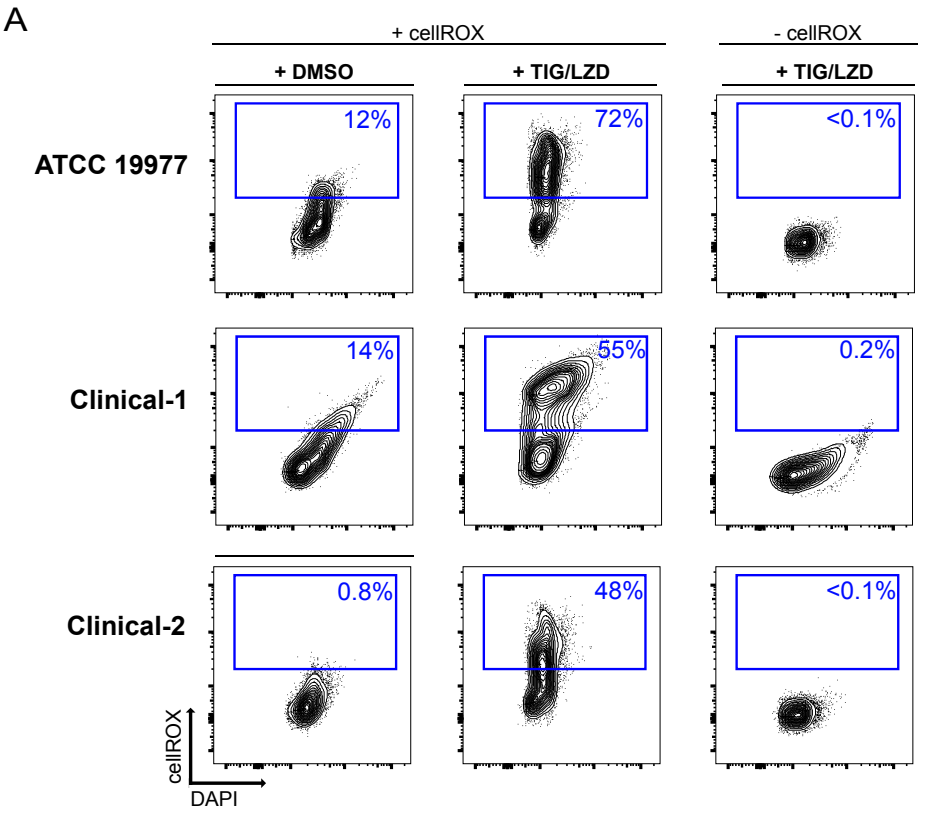
+ cellROX
- cellROX
+ DMSO
+ TIG/LZD
+ TIG/LZD
ATCC 19977
12%
72%
<0.1%
Clinical-1
14%
55%
0.2%
Clinical-2
0.8%
48%
<0.1%
cellROX
DAPI

B

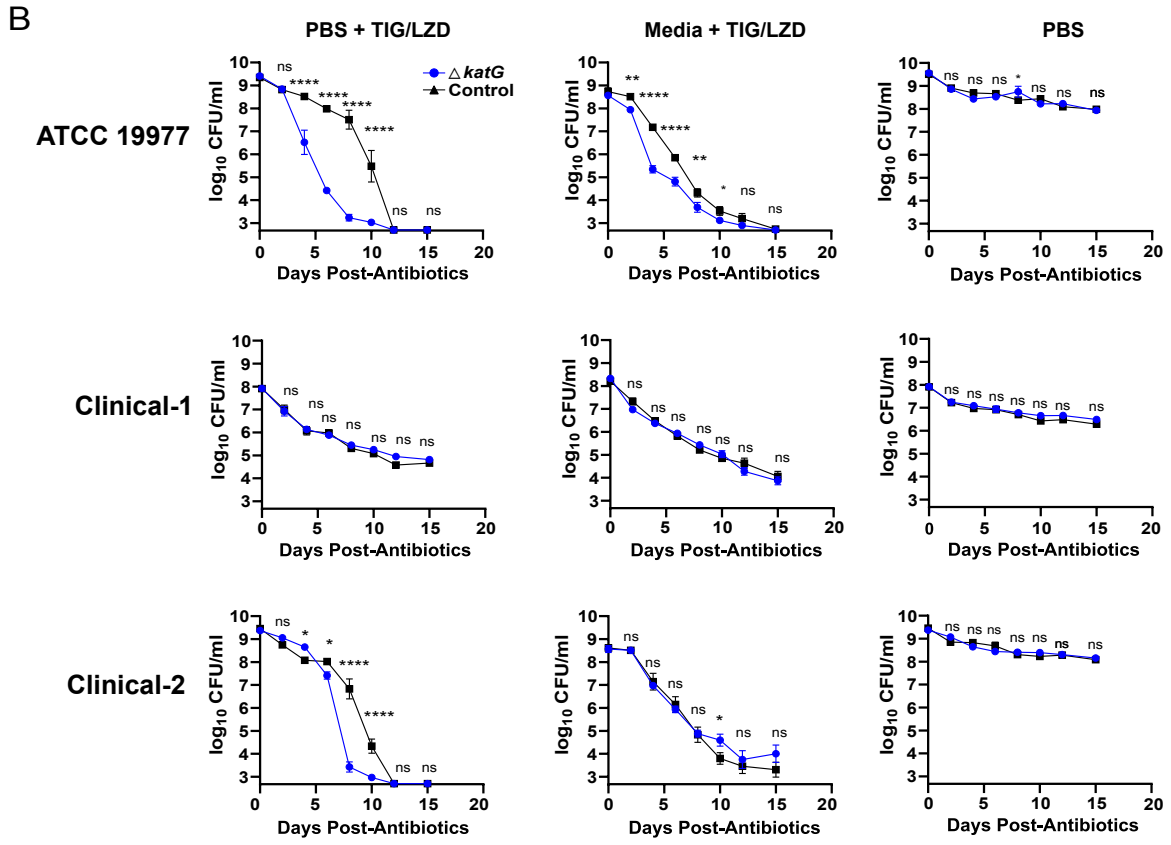
PBS + TIG/LZD
Media + TIG/LZD
PBS
ATCC 19977
Clinical-1
Clinical-2
△ katG
Control
log10 CFU/ml
Days Post-Antibiotics

FIGURE 3: Supplemental

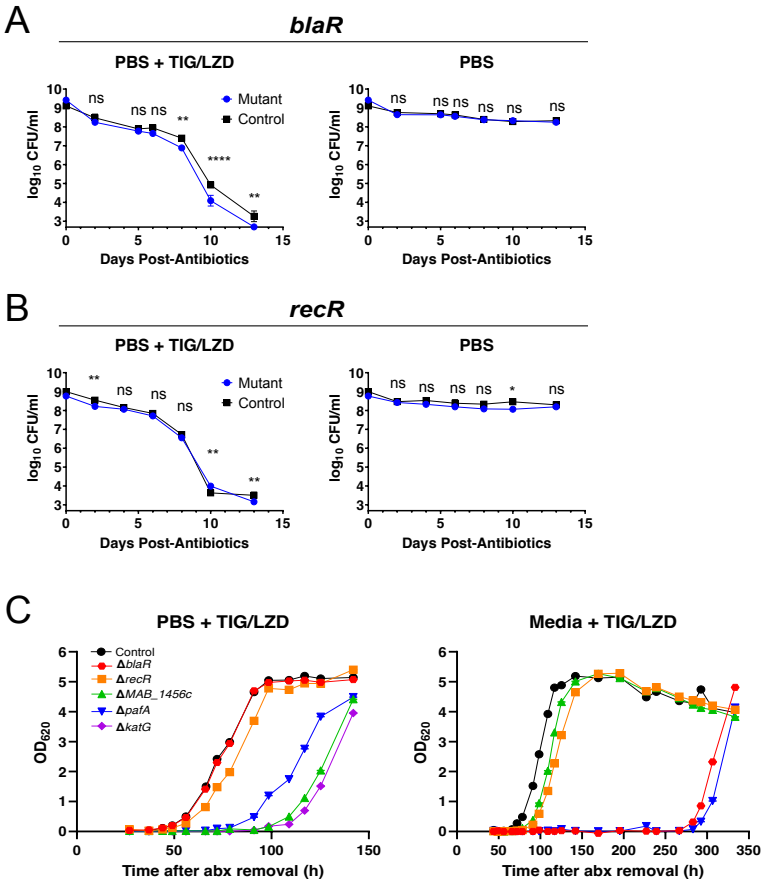
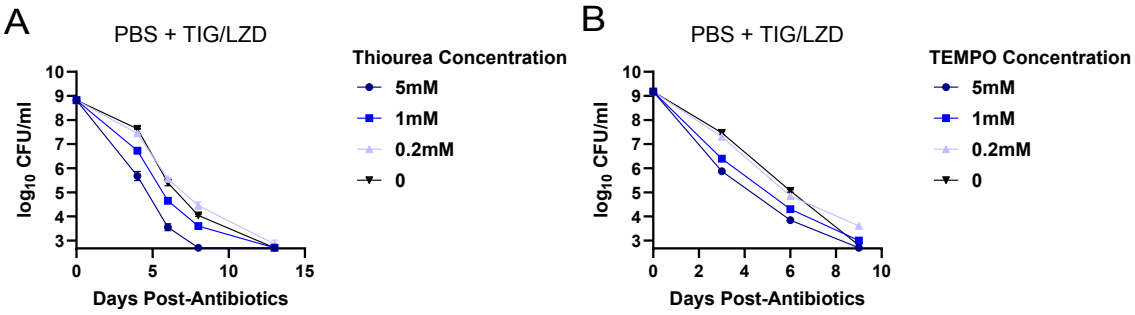
FIGURE 5: Supplemental